Int. J.Nano Dimens. 4(1): 29-49, Summer 2013
ISSN: 2008-8868

Contents list available at **IJND**

International Journal of Nano Dimension

Journal homepage: *www.IJND.ir*

Thermal vibration analysis of double-layer graphene embedded in elastic medium based on nonlocal continuum mechanics

T. J. Prasanna Kumar[1,2,*]
S. Narendar[3,4]
B. L. V. S. Gupta[1]
S. Gopalakrishnan[4]

[1]*Department of Aerospace Engineering, PVP Siddartha Engineering College, Vijayawada 520 007, India.*
[2]*Department of Mechanical Engineering, V. R. Siddhartha Engineering College (Autonomous), Vijayawada 520 007, India.*
[3]*Defence Research and Development Laboratory, Kanchanbagh, Hyderabad 500 058, India.*
[4]*Computational Wave Mechanics Laboratory, Department of Aerospace Engineering, Indian Institute of Science, Bangalore 560 012, India.*

Received 27 August 2012
Accepted 16 November 2012

* Corresponding author:
T. J. Prasanna Kumar
Department of Aerospace Engineering, PVP Siddartha Engineering College, Vijayawada 520 007, India.
Tel +91 9700488731
Fax +91 8885561986
Email tjpk.mech@gmail.com

ABSTRACT

This paper presents the thermal vibration analysis of double-layer graphene sheet embedded in polymer elastic medium, using the plate theory and nonlocal continuum mechanics for small scale effects. The graphene is modeled based on continuum plate theory and the axial stress caused by the thermal effects is also considered. Nonlocal governing equations of motion for this double-layer graphene sheet system are derived from the principle of virtual displacements. The closed form solution for thermal-vibration frequencies of a simply supported rectangular nanoplate has been obtained by using the Navier's method of solution. Numerical results obtained by the present theory are compared with available solutions in the literature and the molecular dynamics results. The influences of the small scale coefficient, the room or low temperature, the high temperature, the half wave number and the aspect ratio of nanoplate on the natural frequencies are considered and discussed in detail. The thermal vibration analysis of single- and double-layer graphene sheets are considered for the analysis. The mode shapes of the respective graphene system are also captured in this work. The present analysis results can be used for the design of the next generation of nanodevices that make use of the thermal vibration properties of the double-layer graphene system..

Keywords: *Graphene; Thermal vibration; Nonlocal Elasticity Theory; Small scale; Mode shape.*

INTRODUCTION

The unique properties of the graphene sheets (GSs) make them very attractive in many scientific research aspects. Some remarkable mechanical properties of GSs reveal that they have potential for creating novel ultra-strength composite materials [1-3]. GSs are mostly used in polymer composites as embedded structures to fortify them [4-6].

Furthermore, the potential applications of the single-layered GSs as mass sensors and atomistic dust detectors have been investigated [7]. Graphite possesses many superior properties [8], such as good electrical and thermal conductivities parallel to the sheets and poor conductivities normal to the sheets, which makes it suitable for gasket material in high temperature or chemical environments; good flexibility, which suggests its use as a vibration damping material; and a high strength-to-weight ratio, which makes it an ideal material for sports equipment. Dubay and Kresse [9] calculated a set of force constants using ab initio density-functional theory, and then calculated the phonon dispersion relation of graphite using these force constants. Their numerical results are in reasonable agreement with the experimental results. Xu and Liao [10] studied the elastic response of a circular single-layered graphene sheets (GSs) under a transverse central load using molecular dynamics, the closed form elasticity solution, and the finite element method. Their simulation gave consistent predictions for the elastic deformation of a GS using molecular dynamics and conventional continuum mechanics. Graphite is composed of multiple layers of GSs that are attracted to each other through the vdW force. It has been reported [11] that single-layered GSs can be detected in carbon nanofilm, but so far single-layered GSs have not been separable from graphite.

Recently, Behfar and Naghdabadi [12] investigated the nanoscale vibration of a multi-layered graphene sheet (MLGS) embedded in an elastic medium, in which the natural frequencies as well as the associated modes were determined using a continuum-based model. The influence of carbon–carbon and carbon–polymer vdW forces are considered in their work. They [13] further studied the bending modulus of a MLGS using a geometrically based analytical approach. The bending energy in their analysis is based on the vdW interactions of atoms belonging to two neighboring sheets. Their calculations are performed for a double-layered GS, but the derived bending modulus is generalized to a MLGS composed of many double-layered GSs along its thickness, in which the double-layered GSs are alternately the same in configuration. In addition, it should be mentioned that graphite is composed of multi-layered sheets, but it was recently reported [11] that single-layered sheet are detectable in carbon nanofilms.

Conducting controlled experiments at the nanoscale is a formidable task while being prohibitively expensive. Therefore, theoretical analyses of nanostructures are still being considered as the dominant tools for modeling such structures. The molecular dynamics (MD) simulations as perhaps the most powerful and reliable approaches are increasingly providing valuable insight into various aspects of nanomaterials and their properties. However, these atomistic simulations are limited to very small length and time scales due to being computationally expensive. Thus, the notions of continuum mechanics have attracted a great deal of attention of many researchers to treat structures at the scale of nanometer. Successful applications of the classical continuum modeling to nanostructured materials have been reported by researchers [12-14]. However, the classical continuum mechanics is scale independent which makes its applicability to the small-scale nanomaterials somewhat questionable. The size effects are recognized to become more pronounced as the dimensions of nanostructures become very small. Hence, the extension of continuum mechanics to accommodate the size dependence of nanomaterials becomes another topic of major concern. Some researchers have proposed the nanoscale continuum theories incorporating interatomic potentials into the continuum model [15, 16]. Application of nonlocal continuum mechanics allowing for the small scale effects to analysis of nanomaterials has been also suggested by some other research workers in the study of nanostructures [17-31]. Herein, some of the most relevant published papers on the nonlocal version of continuum models are cited.

The small scale of nanostructures makes the applicability of classical or local continuum models, such as beam, shell and plate models, questionable. Classical continuum models do not admit intrinsic size dependence in the elastic solutions of inclusions and inhomogeneities. At nanometer scales, however, size effects often become prominent, the cause of which needs to be explicitly addressed due to an increasing interest in the general area of nanotechnology [32]. Sun et al. [33] indicated the importance of a semi-continuum model in analyzing nanomaterials after pointing out

the limitations of the applicability of classical continuum models to nanotechnology. In their semi-continuum model for nanostructured materials with plate like geometry, material properties were found completely dependent on the thickness of the plate structure contrary to classical continuum models. The modeling of such a size-dependent phenomenon has become an interesting research subject in this field. It is thus concluded that the applicability of classical continuum models at very small scales is questionable, since the material microstructure, such as lattice spacing between individual atoms, becomes increasingly important at small size and the discrete structure of the material can no longer be homogeneities into a continuum. Therefore, continuum models need to be extended to consider the scale effect in nanomaterial studies. This can be accomplished through proposing nonlocal continuum mechanics models.

Nonlocal elasticity theory [34-36] was proposed to account for the scale effect in elasticity by assuming the stress at a reference point to be a function of strain field at every point in the body. This way, the internal size scale could be simply considered in constitutive equations as a material parameter only recently has the nonlocal elasticity theory been introduced to nanomaterial applications. As the length scales are reduced, the influences of long-range interatomic and intermolecular cohesive forces on the static and dynamic properties tend to be significant and cannot be neglected. The classical theory of elasticity being the long wave limit of the atomic theory excludes these effects. Thus the traditional classical continuum mechanics would fail to capture the small scale effects when dealing in nano structures. The small size analysis using local theory over predicts the results. Thus the consideration of small effects is necessary for correct prediction of micro/nano structures. Chen et al. [37] proved that the nonlocal continuum theory based models are physically reasonable from the atomistic viewpoint of lattice dynamics and molecular dynamics simulations. However, the most reportedly used continuum theory for analyzing small scale structures is the nonlocal elasticity theory initiated by Eringen [35, 36]. Using this nonlocal elasticity theory, some drawbacks of the classical continuum theory can be efficiently avoided and size-dependent phenomena can be satisfactorily explained. In nonlocal elasticity theory the small scale effects are captured by assuming the stress components at a point is dependent not only on the strain components at the same point but also on all other points in the domain.

The recent work by Pradhan and Phadikar [18] on the vibration analysis of double-layered GSs embedded in a polymer matrix was also based upon the nonlocal continuum mechanics. Pradhan and Phadikar [19] extended their previous research work on the basis of the classic plate theory to the first order shear deformation theory.

For the accurate mechanical analysis of discrete nanostructures, experiments and molecular dynamic simulations are more appropriate. However as controlled experiments in nanoscale are difficult and molecular dynamic simulations are computationally expensive, theoretical modelings of nanostructures become an important issue concerning approximate analysis of nanostructures. Continuum modeling of nanostructures has thus received increased deal of attentions. However classical continuum elasticity, which is a scale-free theory, cannot predict the size effects. In nonlocal elasticity theory the small scale effects are captured by assuming the stress components at a point is dependent not only on the strain components at the same point but also on all other points in the domain. In the literature a great deal of attention has been focused on studying the thermal vibration behavior of one-dimensional nanostructures using nonlocal elasticity theory. These nanostructures include nanobeams, nanorods and carbon nanotubes. On the contrary no work appears related to the thermal-vibration of double layer nanoplates. So, the present work is motivated to analyze the thermal vibration features of the double-layer graphene sheets (DLGSs) embedded in polymer medium based on size dependent nonlocal elasticity theory.

The main objective of the work reported here was to establish a simple and suitable continuum-based model to investigate the vibration behavior of a DLGS that is embedded in an elastic matrix. A set of explicit formulas is derived for the natural frequencies and the associated modes in the special cases of single- and double-layered GSs. These formulae clearly indicate the influence of the van der Waals (vdW) interaction and the surrounding matrix on the vibration behavior. The

effects of the vdW interaction and of the surrounding matrix on the resonant frequency and the associated mode shape are examined in graphical form.

EXPERIMENTAL

Theory of Nonlocal Elasticity

This theory assumes that the stress state at a reference point X in the body is regarded to be dependent not only on the strain state at X but also on the strain states at all other points X' of the body. The most general form of the constitutive relation in the nonlocal elasticity type representation involves an integral over the entire region of interest. The integral contains a nonlocal kernel function, which describes the relative influences of the strains at various locations on the stress at a given location. The constitutive equations of linear, homogeneous, isotropic, non-local elastic solid with zero body forces are given by [36].

$$\sigma_{ij,i} + \rho(f_j - \ddot{u}_j) = 0 \quad \textbf{(1)}$$

$$\sigma_{ij}(\mathbf{X}) = \int_V \alpha(|\mathbf{X} - \mathbf{X}'|, \xi)\sigma_{ij}^c(\mathbf{X}')dV(\mathbf{X}') \quad \textbf{(2)}$$

$$\sigma_{ij}^c(\mathbf{X}') = C_{ijkl}\varepsilon_{kl}(\mathbf{X}') \quad \textbf{(3)}$$

$$\varepsilon_{ij}(\mathbf{X}') = \frac{1}{2}\left(\frac{\partial u_i(\mathbf{X}')}{\partial \mathrm{x}_j'} + \frac{\partial u_j(\mathbf{X}')}{\partial \mathrm{x}_j'}\right) \quad \textbf{(4)}$$

Equation (1) is the equilibrium equation, where $\sigma_{ij,i}$, ρ, f_j and u_j are the stress tensor, mass density, body force density and displacement vector at a reference point $\mathbf{X}$ in the body, respectively, at time t. Equation (3) is the classical constitutive relation where $\sigma_{ij}^c(\mathbf{X}')$ is the classical stress tensor at any point $\mathbf{X}'$ in the body, which is related to the linear strain tensor $\varepsilon_{kl}(\mathbf{X}')$ at the same point. Equation (4) is the classical strain-displacement relationship. The only difference between equations (1)-(4) and the corresponding equations of classical elasticity is the introduction of equation (2), which relates the global (or nonlocal) stress tensor $\sigma_{ij,i}$ to the classical stress tensor $\sigma_{ij}^c(\mathbf{X}')$ using the modulus of nonlocalness. The modulus of nonlocalness or the nonlocal modulus $\alpha(|\mathbf{X} - \mathbf{X}'|, \xi)$ is the kernel of the integral equation (2) and contains parameters which correspond to the nonlocalness [36]. A dimensional analysis of equation (2) clearly shows that the nonlocal modulus has dimensions of $(length)^{-3}$ and so it depends on a characteristic length ratio a/ℓ where a is an internal characteristic length (lattice parameter, size of grain, granular distance, etc.) and ℓ is an external characteristic length of the system (wavelength, crack length, size or dimensions of sample, etc.). Therefore the nonlocal modulus can be written in the following form:

$$\alpha = \alpha(|\mathbf{X} - \mathbf{X}'|, \xi), \quad \xi = \frac{e_0 a}{\ell} \quad \textbf{(5)}$$

where e_0 is a constant appropriate to the material and has to be determined for each material independently [36].

Making certain assumptions [36], the integro-partial differential equations of nonlocal elasticity can be simplified to partial differential equations. For example, equation (2) takes the following simple form:

$$(1 - \xi^2\ell^2\nabla^2)\sigma_{ij}(\mathbf{X}) = \sigma_{ij}^c(\mathbf{X}) = C_{ijkl}\varepsilon_{kl}(\mathbf{X}) \quad \textbf{(6)}$$

where C_{ijkl} is the elastic modulus tensor of classical isotropic elasticity and ε_{ij} is the strain tensor, ∇^2 denotes the second order spatial gradient applied on the stress tensor σ_{ij} and $\xi = e_0 a/\ell$.

A method of identifying the small scaling parameter e_0 in the nonlocal theory is not known yet. As defined by Eringen [36], e_0 is a constant appropriate to each material. Eringen proposed $e_0 = \frac{\sqrt{\pi^2-4}}{2\pi} \cong 0.39$ by the matching of the dispersion curves via nonlocal theory for plane wave and Born-Karman model of lattice dynamics at the end of the Brillouin zone ($ka = \pi$), where a is the distance between atoms and k is the wavenumber in the phonon analysis [36]. According to Sudak [38], values of e_0 need to be determined from experimental results, and in the results of Sudak [38], it was concluded that L/a (L is the length of CNT) and e_0 should be the same order or one order less to have any significant nonlocal effect. Zhang et al. [39] approximated that

$e_0 \approx 0.82$ by matching the theoretical buckling strain obtained by the nonlocal elastic cylindrical shell model using Donell theory to those from molecular mechanics simulations given by Sears and Batra [40]. By using the strain gradient approach, the parameter e_0 was proposed that $e_0 \approx 0.288$ by Wang and Hu [41]. The above-mentioned studies clearly indicate that reasonable choice of the value of the parameter e_0 a is crucial to ensure the validity of the nonlocal models, and therefore more works are required to determine the value of e_0 a more accurately for nanostructures. A conservative estimate of the nonlocal parameter $0 \leq e_0 a \leq 2.0\ nm$ for a single walled carbon nanotube is proposed by Wang [42].

Recently, Narendar et al. [43] presented an expression for the non-local scaling parameter as a function of the geometric and electronic properties of single-walled CNTs. A self-consistent method was developed for the linearization of the problem of ultrasonic wave propagation in CNTs. They proved that (a) the general three-dimensional elastic problem leads to a single non-local scaling parameter (e_0), (b) e_0 is almost constant irrespective of chirality of CNT in the case of longitudinal wave propagation, (c) e_0 is a linear function of diameter of CNT for the case of torsional mode of wave propagation, and (d) e_0 in the case of coupled longitudinal-torsional modes of wave propagation, is a function which exponentially converges to that of axial mode at large diameters and to torsional mode at smaller diameters. Narendar and Gopalakrishnan [44] also recommended the value of the scale coefficient to be about 0.11 nm for the application of the nonlocal theory in the analysis of axial compression of carbon nanotubes.

Therefore, in this study, the nonlocal parameter is taken as $e_0 a = 0\ and\ 0.5\ nm$ to investigate nonlocal effects on the terahertz wave characteristics of a monolayer graphene.

Nonlocal Governing Partial Differential Equations for Monolayer Graphene Sheet

Figure 1(a) shows a rectangular graphene sheet and its equivalent continuum model. Liew et al. [45] considered graphene as isotropic material in their continuum model. In the present work such continuum plate model has been assumed. The coordinate system used for the graphene sheet is shown in Figure 1. Origin is chosen at one corner of the plate. The x coordinate of the axis is taken along the length of the plate, y coordinate is taken along the width of the plate and z coordinate is taken along the thickness of the plate. The displacement field according to classical plate theory (CLPT) can be written as [46]

$$u_1(x,y,z,t) = u(x,y,t) - z\frac{\partial w(x,y,t)}{\partial x}$$

$$u_2(x,y,z,t) = v(x,y,t) - z\frac{\partial w(x,y,t)}{\partial y}$$

$$u_3(x,y,z,t) = w(x,y,t) \qquad \textbf{(7a,b,c)}$$

Here u, v and w denote displacement along x, y and z directions, respectively (see Figure 1). The strains can be calculated as

$$\varepsilon_{xx} = \frac{\partial u_1}{\partial x} = \frac{\partial u}{\partial x} - z\frac{\partial^2 w}{\partial x^2}$$

$$\varepsilon_{yy} = \frac{\partial u_2}{\partial y} = \frac{\partial v}{\partial y} - z\frac{\partial^2 w}{\partial y^2}$$

$$\gamma_{xy} = \frac{\partial u_1}{\partial y} + \frac{\partial u_2}{\partial x} = \frac{\partial u}{\partial y} + \frac{\partial v}{\partial x} - 2z\frac{\partial^2 w}{\partial x\,\partial y}$$

$$\varepsilon_{zz} = 0, \quad \gamma_{xz} = 0, \quad \gamma_{yz} = 0 \qquad \textbf{(8-a,b,c,d)}$$

It can be noted that nonlocal behavior enters through the constitutive relations. Principle of virtual work is independent of constitutive relations. So this can be applied to derive the equilibrium equations of the nonlocal plates.

Using the principle of virtual work, following equilibrium equation in w can be obtained [28]

$$\frac{\partial^2 M_{xx}}{\partial x^2} + 2\frac{\partial^2 M_{xy}}{\partial x\,\partial y} + \frac{\partial^2 M_{yy}}{\partial y^2} + \frac{E\alpha\Delta T}{1-\nu}\mathrm{t}\left(\frac{\partial^2 w}{\partial x^2} + \frac{\partial^2 w}{\partial x^{2\,\partial y^2}} + \frac{\partial^2 w}{\partial y^2}\right) = \mathrm{J}_0\frac{\partial^2 \mathrm{w}}{\partial \mathrm{t}^2} - \mathrm{J}_2\left(\frac{\partial^4 \mathrm{w}}{\partial \mathrm{x}^2\,\partial \mathrm{t}^2} + \frac{\partial^4 \mathrm{w}}{\partial \mathrm{y}^2\,\partial \mathrm{t}^2}\right)$$

(9)

where J_0 and J_2 are mass moments of inertia and are defined as follows

$$J_0 = \int_{-\frac{t}{2}}^{+\frac{t}{2}} \rho z dz, \qquad J_2 = \int_{-\frac{t}{2}}^{+\frac{t}{2}} \rho z^2 dz \qquad \textbf{(10-a,b)}$$

Here t denotes the thickness of the plate and the moment resultants

$$M_{xx} = \int_{-\frac{t}{2}}^{+\frac{t}{2}} z\sigma_{xx} dz$$

$$M_{xy} = \int_{-\frac{t}{2}}^{+\frac{t}{2}} z\tau_{xy} dz$$

$$M_{yy} = \int_{-\frac{t}{2}}^{+\frac{t}{2}} z\sigma_{yy} dz \qquad \textbf{(11-a,b,c)}$$

Using Eq. ((6)), the plane stress constitutive relation of a nonlocal plate becomes

$$\begin{Bmatrix}\sigma_{xx}\\ \sigma_{yy}\\ \tau_{xy}\end{Bmatrix} - g^2\left[\frac{\partial^2}{\partial x^2} + \frac{\partial^2}{\partial y^2}\right]\begin{Bmatrix}\sigma_{xx}\\ \sigma_{yy}\\ \tau_{xy}\end{Bmatrix} = \begin{bmatrix}C_{11} & C_{12} & 0\\ C_{21} & C_{22} & 0\\ 0 & 0 & C_{66}\end{bmatrix}\begin{Bmatrix}\varepsilon_{xx}\\ \varepsilon_{yy}\\ \gamma_{xy}\end{Bmatrix} + \begin{Bmatrix}-\frac{E\alpha\Delta T}{1-\nu}\\ -\frac{E\alpha\Delta T}{1-\nu}\\ 0\end{Bmatrix}$$

(12)

where, σ_{xx} and σ_{yy} are the normal stresses in x and y directions respectively and τ_{xy} is the in-plane shear stress. For the case of an isotropic plate, the expressions for C_{ij} in terms of Young's modulus E and Poisson's ratio ν are given as $C_{11} = C_{22} = \frac{E}{1-\nu^2}$, $C_{12} = C_{21} = \frac{\nu E}{1-\nu^2}$ and $C_{66} = \frac{E}{2(1+\nu)}$ and $g = e_0 a$ is the nonlocal scale parameter.

Using strain displacement relationship (Eq. (8)), stress-strain relationship (Eq. (12)) and stress resultants definition (Eq. (11)), we can express stress resultants in terms of displacements as follows

$$M_{xx} - g^2\left(\frac{\partial^2 M_{xx}}{\partial x^2} + \frac{\partial^2 M_{xx}}{\partial y^2}\right) = -\mathrm{D}\left(\frac{\partial^2 w}{\partial x^2} + \frac{\partial^2 w}{\partial y^2}\right) - \int_{-t/2}^{t/2} \frac{E\alpha\Delta T z}{1-\nu} dz$$

$$M_{xy} - g^2\left(\frac{\partial^2 M_{xy}}{\partial x^2} + \frac{\partial^2 M_{xy}}{\partial y^2}\right) = -2\mathrm{D}\frac{\partial^2 w}{\partial x\,\partial y} - \int_{-t/2}^{t/2} \frac{E\alpha\Delta T z}{1-\nu} dz$$

$$M_{yy} - g^2\left(\frac{\partial^2 M_{yy}}{\partial x^2} + \frac{\partial^2 M_{yy}}{\partial y^2}\right) = -\mathrm{D}\left(\frac{\partial^2 w}{\partial x^2} + \frac{\partial^2 w}{\partial y^2}\right) \qquad \textbf{(13-a,b,c)}$$

where

$$D = C_{11} I_2, \quad \mathrm{I}_2 = \int_{-\frac{t}{2}}^{+\frac{t}{2}} z^2 dz \qquad \textbf{(14)}$$

Using Eqs. (9) and (13) we get the following nonlocal governing partial differential equation in terms of flexural displacement w

$$\mathrm{D}\left(\frac{\partial^4 w}{\partial x^4} + 2\frac{\partial^4 w}{\partial x^2\,\partial y^2} + \frac{\partial^4 w}{\partial y^4}\right) - N_{th}\left(\frac{\partial^2 w}{\partial x^2} + \frac{\partial^2 w}{\partial y^2}\right) + N_{th}g^2\left(\frac{\partial^4 w}{\partial x^4} + 2\frac{\partial^4 w}{\partial x^2\partial y^2} + \frac{\partial^4 w}{\partial y^4}\right) - J_0 g^2\left(\frac{\partial^4 w}{\partial x^2\,\partial t^2} + \frac{\partial^4 w}{\partial y^2\,\partial t^2}\right) + J_2 g^2\left(\frac{\partial^6 w}{\partial x^4\,\partial t^2} + 2\frac{\partial^6 w}{\partial x^2\,\partial y^2\,\partial t^2} + \frac{\partial^6 w}{\partial y^4\,\partial t^2}\right) + J_0\frac{\partial^2 w}{\partial t^2} - J_2\left(\frac{\partial^4 w}{\partial x^2\,\partial t^2} + \frac{\partial^4 w}{\partial y^2\,\partial t^2}\right) = 0$$

(15)

Nanoscale Modelling of DLGS embedded in Elastic Matrix: Governing Equations

In order to determine the natural frequencies of a multi-layered graphene sheet, it is assumed that the layers behave like general form of isotropic plates stacking at the top of each other and bonding with van der Waals forces. Such assumption is based on the difference between the elastic moduli in two orientations of the sheet. For a simply supported plate, boundary conditions are considered somehow the components of in-plane forces in the equation of motion are dropped and merely bending components remain. The deflections of neighboring layers are coupled through the *van der Waals* interaction between any two adjacent ones. For small-deflection of the graphene sheet, it is assumed that the interaction pressure at any point between adjacent sheets linearly depends on the difference of their deflections. Thus transverse motion of N neighboring graphene sheets is described by N coupled equations as:

$$
\begin{aligned}
&\mathrm{D}\left(\frac{\partial^4 w_1}{\partial x^4}+2\frac{\partial^4 w_1}{\partial x^2\,\partial y^2}+\frac{\partial^4 w_1}{\partial y^4}\right)-N_{th}\left(\frac{\partial^2 w_1}{\partial x^2}+\frac{\partial^2 w_1}{\partial y^2}\right)+N_{th}g^2\left(\frac{\partial^4 w_1}{\partial x^4}+2\frac{\partial^4 w_1}{\partial x^2\partial y^2}+\frac{\partial^4 w_1}{\partial y^4}\right)\\
&\quad -J_0 g^2\left(\frac{\partial^4 w_1}{\partial x^2\,\partial t^2}+\frac{\partial^4 w_1}{\partial y^2\,\partial t^2}\right)+J_2 g^2\left(\frac{\partial^6 w_1}{\partial x^4\,\partial t^2}+2\frac{\partial^6 w_1}{\partial x^2\,\partial y^2\,\partial t^2}+\frac{\partial^6 w_1}{\partial y^4\,\partial t^2}\right)+J_0\frac{\partial^2 w_1}{\partial t^2}\\
&\quad -J_2\left(\frac{\partial^4 w_1}{\partial x^2\,\partial t^2}+\frac{\partial^4 w_1}{\partial y^2\,\partial t^2}\right)\\
&\quad =\mathrm{F}_1+C_{12}(w_2-w_1)-g^2\left(\frac{\partial^2 F_1}{\partial x^2}+\frac{\partial^2 F_1}{\partial y^2}\right)-C_{12}g^2\left(\frac{\partial^2 w_2}{\partial x^2}+\frac{\partial^2 w_2}{\partial y^2}-\frac{\partial^2 w_1}{\partial x^2}-\frac{\partial^2 w_1}{\partial y^2}\right)\\
&\mathrm{D}\left(\frac{\partial^4 w_2}{\partial x^4}+2\frac{\partial^4 w_2}{\partial x^2\,\partial y^2}+\frac{\partial^4 w_2}{\partial y^4}\right)-N_{th}\left(\frac{\partial^2 w_2}{\partial x^2}+\frac{\partial^2 w_2}{\partial y^2}\right)+N_{th}g^2\left(\frac{\partial^4 w_2}{\partial x^4}+2\frac{\partial^4 w_2}{\partial x^2\partial y^2}+\frac{\partial^4 w_2}{\partial y^4}\right)\\
&\quad -J_0 g^2\left(\frac{\partial^4 w_2}{\partial x^2\,\partial t^2}+\frac{\partial^4 w_2}{\partial y^2\,\partial t^2}\right)+J_2 g^2\left(\frac{\partial^6 w_2}{\partial x^4\,\partial t^2}+2\frac{\partial^6 w_2}{\partial x^2\,\partial y^2\,\partial t^2}+\frac{\partial^6 w_2}{\partial y^4\,\partial t^2}\right)+J_0\frac{\partial^2 w_2}{\partial t^2}\\
&\quad -J_2\left(\frac{\partial^4 w_2}{\partial x^2\,\partial t^2}+\frac{\partial^4 w_2}{\partial y^2\,\partial t^2}\right)\\
&\quad =\mathrm{F}_2-C_{12}(w_2-w_1)-g^2\left(\frac{\partial^2 F_2}{\partial x^2}+\frac{\partial^2 F_2}{\partial y^2}\right)+C_{12}g^2\left(\frac{\partial^2 w_2}{\partial x^2}+\frac{\partial^2 w_2}{\partial y^2}-\frac{\partial^2 w_1}{\partial x^2}-\frac{\partial^2 w_1}{\partial y^2}\right)
\end{aligned}
\tag{16}
$$

Where $w_i(x,y,t)$, $i=1,2$ is the deflection of the i^{th} graphene sheet; $i=1$ denotes the one side outermost graphene sheet and $i=2$, the other side outermost graphene sheet. F is the pressure per unit area, acting on both outermost graphene sheets due to the surrounding elastic medium and C_{ij} is the carbon–carbon van der Waals interaction coefficient.

The pressure that is exerted on sheet i due to the vdW interaction between layers (q_i) and D is the bending stiffness of the individual sheet. We only consider infinitesimal vibration, and thus the net pressure due to the vdW interaction is assumed to be linearly proportional to the deflection between two layers. Consider the DLGS as shown in Figure 1. The two graphene sheets of the DLGS are referred to as GS-1 and GS-2. The GSs are considered to be of thickness$h$. Vertically distributed springs couples the two GSs. The springs may be used to substitute the electrostatic force, elastic medium, van der Waals forces or forces due to optomechanical coupling between the two GSs.

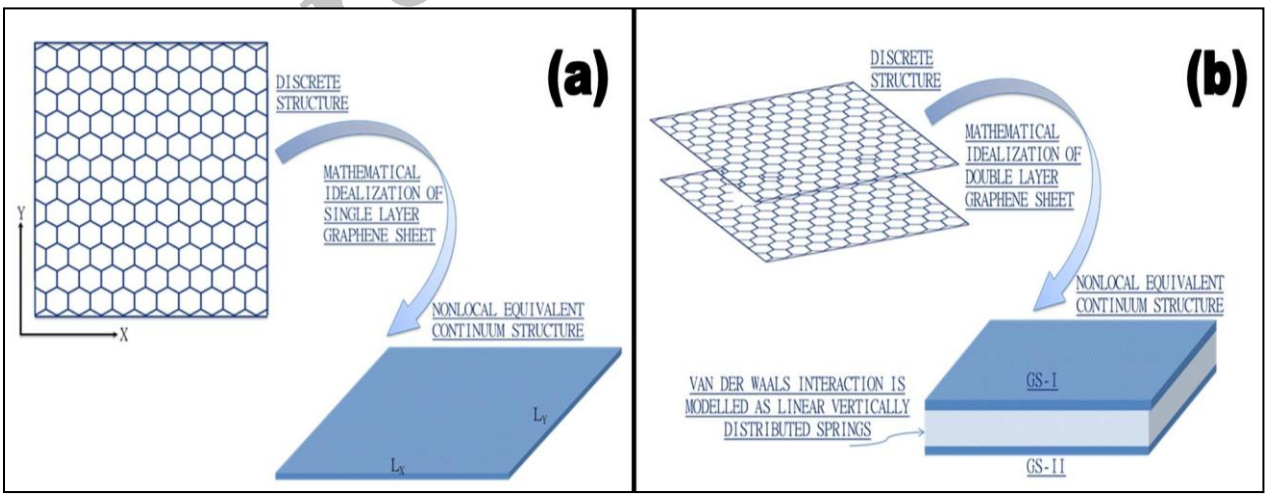

Fig. 1. Mathematical idealization of (a) single layer graphene sheet and (b) double layer graphene sheet.

The equilibrium distance between GSs is around 0.34 nm, and thus the initial pressure between layers can be ignored if the initial interlayer space is taken as 0.34 nm. As infinitesimal deformation is considered, the pressure can be assumed to be linearly proportional to the deflection between two graphene layers:

$$q_i = \sum_{j=1}^{N} \mathrm{C_{ij}}(\mathrm{w_i} - \mathrm{w_j}) \qquad \textbf{(17)}$$

where the coefficients $\mathrm{C_{ij}}$ are given by

$$\mathrm{C_{ij}} = -\left(\frac{4\sqrt{3}}{9a}\right)^2 \frac{24\varepsilon}{\sigma^2}\left(\frac{\sigma}{a}\right)^8 \left[\frac{3003\pi}{256}\sum_{k=0}^{5}\frac{(-1)^k}{2k+1}\binom{5}{k}\left(\frac{\sigma}{a}\right)^6 \frac{1}{(\bar{z}_i - \bar{z}_j)^{12}} - \frac{35\pi}{8}\sum_{k=0}^{2}\frac{(-1)^k}{2k+1}\binom{2}{k}\frac{1}{(\bar{z}_i - \bar{z}_j)^6}\right]$$

(18)

where N is the total number of layers of the multi-layer graphene sheet (MLGS), $a = 1.42\text{Å}$ is the C –C bond length, $\bar{z}_i = \frac{z_i}{a}$ (where z_i is the coordinate of the i^{th} layer in the thickness direction with the origin at the mid-plane of the GSs), and ε and σ are parameters that are chosen to fit the physical properties of the material. The values of interaction coefficients for the present three-layer graphene system are calculate and are given in Table 1.

Table 1. van der Waals (vdW) interaction coefficients C_{ij} $(GPa\ nm^{-1})$ between layers i and j of a double-layered graphene sheet

Number of layers (N)	$j = 1$	$j = 2$
$i = 1$	0	-108.651
$i = 2$	-108.651	0

Nonlocal governing equations of single layer graphene sheet embedded in polymer medium

A single-layered rectangular GS embedded in an elastic medium (polymer matrix) is considered. The chemical bonds are assumed to be formed between the GSs and the elastic medium. The polymer matrix is described by a Pasternak foundation model, which accounts for both normal pressure and the transverse shear deformation of the surrounding elastic medium. When the shear effects are neglected, the model reduces to Winkler foundation model. The normal pressure or Winkler elastic foundation parameter is approximated as a series of closely spaced, mutually independent, vertical linear elastic springs where the foundation modulus is assumed equivalent to stiffness of the springs. The normal pressure and the incompressible layer that resists transverse shear deformation by Winkler and Pasternak foundation model are expressed as

$$F_{Winkler} = -K_W w \qquad \textbf{(19)}$$

$$F_{Pasternak} = -K_S w + K_G\left(\frac{\partial^2 w}{\partial x^2} + \frac{\partial^2 w}{\partial y^2}\right) \qquad \textbf{(20)}$$

where K_W and K_G denote the Winkler modulus parameter and the shear modulus of the surrounding medium, respectively.

The nonlocal governing equation of single layer graphene sheet embedded in polymer elastic medium under thermal loading is given as:

$$\mathrm{D}\left(\frac{\partial^4 w_1}{\partial x^4} + 2\frac{\partial^4 w_1}{\partial x^2\,\partial y^2} + \frac{\partial^4 w_1}{\partial y^4}\right) - N_{th}\left(\frac{\partial^2 w_1}{\partial x^2} + \frac{\partial^2 w_1}{\partial y^2}\right) + N_{th}g^2\left(\frac{\partial^4 w_1}{\partial x^4} + 2\frac{\partial^4 w_1}{\partial x^2\partial y^2} + \frac{\partial^4 w_1}{\partial y^4}\right) - J_0 g^2\left(\frac{\partial^4 w_1}{\partial x^2\,\partial t^2} + \frac{\partial^4 w_1}{\partial y^2\,\partial t^2}\right) + J_2 g^2\left(\frac{\partial^6 w_1}{\partial x^4\,\partial t^2} + 2\partial 6w1\partial x2\partial y2\partial t2 + \partial 6w1\partial y4\partial t2 + \partial 02w1\partial t2 - \partial 2\partial 4w1\partial x2\partial t2 + \partial 4w1\partial y2\partial t2 = \mathrm{F_1} - g^2\left(\frac{\partial^2 F_1}{\partial x^2} + \frac{\partial^2 F_1}{\partial y^2}\right)\right)$$

(21)

or

$$\begin{aligned}\mathrm{D}\left(\frac{\partial^4 w_1}{\partial x^4} + 2\frac{\partial^4 w_1}{\partial x^2\,\partial y^2} + \frac{\partial^4 w_1}{\partial y^4}\right) - N_{th}\left(\frac{\partial^2 w_1}{\partial x^2} + \frac{\partial^2 w_1}{\partial y^2}\right) &+ N_{th}g^2\left(\frac{\partial^4 w_1}{\partial x^4} + 2\frac{\partial^4 w_1}{\partial x^2\partial y^2} + \frac{\partial^4 w_1}{\partial y^4}\right) \\ &- J_0 g^2\left(\frac{\partial^4 w_1}{\partial x^2\,\partial t^2} + \frac{\partial^4 w_1}{\partial y^2\,\partial t^2}\right) \\ &+ J_2 g^2\left(\frac{\partial^6 w_1}{\partial x^4\,\partial t^2} + 2\frac{\partial^6 w_1}{\partial x^2\,\partial y^2\,\partial t^2} + \frac{\partial^6 w_1}{\partial y^4\,\partial t^2}\right) \\ &+ J_0\frac{\partial^2 w_1}{\partial t^2} - J_2\left(\frac{\partial^4 w_1}{\partial x^2\,\partial t^2} + \frac{\partial^4 w_1}{\partial y^2\,\partial t^2}\right) \\ &= -K_S w_1 + K_G\left(\frac{\partial^2 w_1}{\partial x^2} + \frac{\partial^2 w_1}{\partial y^2}\right) \\ &+ g^2 K_S\left(\frac{\partial^2 w_1}{\partial x^2} + \frac{\partial^2 w_1}{\partial y^2}\right) \\ &- K_G g^2\left(\frac{\partial^4 w_1}{\partial x^4} + 2\frac{\partial^4 w_1}{\partial x^2\,\partial y^2} + \frac{\partial^4 w_1}{\partial y^4}\right)\end{aligned}$$

(22)

Nonlocal governing equations of double layer graphene sheet embedded in polymer medium

The nonlocal governing equation of double layer graphene sheet embedded in polymer elastic medium under thermal loading is given as:

Layer-1

$$\mathrm{D}\left(\frac{\partial^4 w_1}{\partial x^4}+2\frac{\partial^4 w_1}{\partial x^2\,\partial y^2}+\frac{\partial^4 w_1}{\partial y^4}\right)-N_{th}\left(\frac{\partial^2 w_1}{\partial x^2}+\frac{\partial^2 w_1}{\partial y^2}\right)+N_{th}g^2\left(\frac{\partial^4 w_1}{\partial x^4}+2\frac{\partial^4 w_1}{\partial x^2\partial y^2}+\frac{\partial^4 w_1}{\partial y^4}\right)-J_0g^2\left(\frac{\partial^4 w_1}{\partial x^2\,\partial t^2}+\frac{\partial^4 w_1}{\partial y^2\,\partial t^2}\right)+J_2g^2\left(\frac{\partial^6 w_1}{\partial x^4\,\partial t^2}+2\frac{\partial^6 w_1}{\partial x^2\,\partial y^2\,\partial t^2}+\frac{\partial^6 w_1}{\partial y^4\,\partial t^2}\right)+J_0\frac{\partial^2 w_1}{\partial t^2}-J_2\left(\frac{\partial^4 w_1}{\partial x^2\,\partial t^2}+\frac{\partial^4 w_1}{\partial y^2\,\partial t^2}\right)=-K_S w_1+K_G\left(\frac{\partial^2 w_1}{\partial x^2}+\frac{\partial^2 w_1}{\partial y^2}\right)+C_{12}(w_2-w_1)+g^2K_S\left(\frac{\partial^2 w_1}{\partial x^2}+\frac{\partial^2 w_1}{\partial y^2}\right)-K_Gg^2\left(\frac{\partial^4 w_1}{\partial x^4}+2\frac{\partial^4 w_1}{\partial x^2\,\partial y^2}+\frac{\partial^4 w_1}{\partial y^4}\right)-C_{12}g^2\left(\frac{\partial^2 w_2}{\partial x^2}+\frac{\partial^2 w_2}{\partial y^2}-\frac{\partial^2 w_1}{\partial x^2}-\frac{\partial^2 w_1}{\partial y^2}\right)$$

(23)

Layer-2

$$\mathrm{D}\left(\frac{\partial^4 w_2}{\partial x^4}+2\frac{\partial^4 w_2}{\partial x^2\,\partial y^2}+\frac{\partial^4 w_2}{\partial y^4}\right)-N_{th}\left(\frac{\partial^2 w_2}{\partial x^2}+\frac{\partial^2 w_2}{\partial y^2}\right)+N_{th}g^2\left(\frac{\partial^4 w_2}{\partial x^4}+2\frac{\partial^4 w_2}{\partial x^2\partial y^2}+\frac{\partial^4 w_2}{\partial y^4}\right)-J_0g^2\left(\frac{\partial^4 w_2}{\partial x^2\,\partial t^2}+\frac{\partial^4 w_2}{\partial y^2\,\partial t^2}\right)+J_2g^2\left(\frac{\partial^6 w_2}{\partial x^4\,\partial t^2}+2\frac{\partial^6 w_2}{\partial x^2\,\partial y^2\,\partial t^2}+\frac{\partial^6 w_2}{\partial y^4\,\partial t^2}\right)+J_0\frac{\partial^2 w_2}{\partial t^2}-J_2\left(\frac{\partial^4 w_2}{\partial x^2\,\partial t^2}+\frac{\partial^4 w_2}{\partial y^2\,\partial t^2}\right)=-K_S w_1+K_G\left(\frac{\partial^2 w_1}{\partial x^2}+\frac{\partial^2 w_1}{\partial y^2}\right)-C_{12}(w_2-w_1)+g^2K_S\left(\frac{\partial^2 w_1}{\partial x^2}+\frac{\partial^2 w_1}{\partial y^2}\right)-K_Gg^2\left(\frac{\partial^4 w_1}{\partial x^4}+2\frac{\partial^4 w_1}{\partial x^2\,\partial y^2}+\frac{\partial^4 w_1}{\partial y^4}\right)+C_{12}g^2\left(\frac{\partial^2 w_2}{\partial x^2}+\frac{\partial^2 w_2}{\partial y^2}-\frac{\partial^2 w_1}{\partial x^2}-\frac{\partial^2 w_1}{\partial y^2}\right)$$

(24)

Equations (23) and (24) represent the complete governing equations of the double layer nanoplate system under consideration with thermal and small scale effects.

Solution of Governing Equations: Thermal Vibration Analysis

The thermal vibration analysis formulation begins by assuming a solution of the displacement field. In particular, time harmonic waves are sought and it is assumed that the model is unbounded in $Y-$direction (although bounded in $X-$direction). Thus the assumed form is a combination of Fourier transform in $Y-$direction and Fourier transform in time

$$w(x,y,t)=\sum_{m=1}^{\infty}\sum_{n=1}^{\infty}W_{mn}\sin(\lambda_m x)\,sin(\lambda_n y)e^{-i\omega_{\mathrm{mn}}t}$$

(25)

The ω_{mn} is the circular frequency and m, n are the wavenumbers along X and Y directions, respectively and$j=\sqrt{-1}$. Here $\lambda_m=m\pi/L_x$ and $\lambda_n=n\pi/L_y$.

For Single Layer Graphene Sheet Embedded In Elastic Medium

Substituting $w_1(x,y,t)=\sum_{m=1}^{\infty}\sum_{n=1}^{\infty}W_{1_{mn}}\sin(\lambda_m x)\,sin(\lambda_n y)e^{-i\omega_{\mathrm{mn}}t}$ in Equation (22), leads to

$$\begin{aligned}\{(D+N_{th}g^2)(\lambda_m^2+\lambda_n^2)^2+&N_{th}(\lambda_m^2+\lambda_n^2)-J_0\omega^2\\&-J_2\omega^2(\lambda_m^2+\lambda_n^2)-g^2J_0\omega^2(\lambda_m^2+\lambda_n^2)\\&-J_2g^2\omega^2(\lambda_m^2+\lambda_n^2)^2\}W_{1_{mn}}\\&=\{-K_S-K_G(\lambda_m^2+\lambda_n^2)-g^2K_S(\lambda_m^2+\lambda_n^2)\\&-K_Gg^2(\lambda_m^2+\lambda_n^2)^2\}W_{1_{mn}}\end{aligned}$$

(26)

For non-trivial solution of $W_{1_{mn}}$, the above equation can be written as

$$\begin{aligned}(D+N_{th}g^2)(\lambda_m^2+\lambda_n^2)^2+&N_{th}(\lambda_m^2+\lambda_n^2)-J_0\omega^2\\&-J_2\omega^2(\lambda_m^2+\lambda_n^2)-g^2J_0\omega^2(\lambda_m^2+\lambda_n^2)\\&-J_2g^2\omega^2(\lambda_m^2+\lambda_n^2)^2\\&=-K_S-K_G(\lambda_m^2+\lambda_n^2)-g^2K_S(\lambda_m^2+\lambda_n^2)\\&-K_Gg^2(\lambda_m^2+\lambda_n^2)^2\end{aligned}$$

(27a)

This implies

$$\begin{aligned}\Longrightarrow[J_0+J_2(\lambda_m^2+\lambda_n^2)&+J_0g^2(\lambda_m^2+\lambda_n^2)\\&+J_2g^2(\lambda_m^2+\lambda_n^2)^2]\omega^2\\&=(D+N_{th}g^2)(\lambda_m^2+\lambda_n^2)^2\\&+(N_{th}+g^2K_{cs})(\lambda_m^2+\lambda_n^2)+K_S\Gamma_{mn}\\&+K_G(\lambda_m^2+\lambda_n^2)\Gamma_{mn}\end{aligned}$$

(27b)

Now, this relation is solved for natural frequencies of the SLGS as

$$\omega^2=\frac{D(\lambda_m^2+\lambda_n^2)^2+N_{th}\Gamma_{mn}(\lambda_m^2+\lambda_n^2)+K_{cs}\Gamma_{mn}+K_G(\lambda_m^2+\lambda_n^2)\Gamma_{mn}}{J_0\Gamma_{mn}+J_2(\lambda_m^2+\lambda_n^2)\Gamma_{mn}}$$

(27c)

Where $\Gamma_{mn}=1+g^2(\lambda_m^2+\lambda_n^2)$ **(28)**

It can be seen that the frequencies are mainly function of the mode numbers and the nonlocal scale parameter. The effect of these parameters on the frequency of SLGS is discussed in the next section.

Double Layer Graphene Embedded In Elastic Medium

Substituting

$w_1(x,y,t) = \sum_{m=1}^{\infty}\sum_{n=1}^{\infty} W_{1_{mn}} \sin(\lambda_m x)\, sin(\lambda_n y) e^{-i\omega_{mn}t}$

in Equations (23) and (24), leads to

$$\begin{aligned}\{(D+N_{th}g^2)(\lambda_m^2+\lambda_n^2)^2 &+N_{th}(\lambda_m^2+\lambda_n^2)-J_0\omega^2\\ &-J_2\omega^2(\lambda_m^2+\lambda_n^2)-g^2J_0\omega^2(\lambda_m^2+\lambda_n^2)\\ &-J_2g^2\omega^2(\lambda_m^2+\lambda_n^2)^2\}W_{1_{mn}}\\ &=\{-C_{12}-K_S-K_G(\lambda_m^2+\lambda_n^2)\\ &-g^2K_S(\lambda_m^2+\lambda_n^2)-K_Gg^2(\lambda_m^2+\lambda_n^2)^2\\ &-C_{12}(\lambda_m^2+\lambda_n^2)\}W_{1_{mn}}\\ &+\{C_{12}+C_{12}(\lambda_m^2+\lambda_n^2)\}W_{2_{mn}}\end{aligned}$$

(29)

$$\begin{aligned}\{(D+N_{th}g^2)(\lambda_m^2+\lambda_n^2)^2 &+N_{th}(\lambda_m^2+\lambda_n^2)-J_0\omega^2\\ &-J_2\omega^2(\lambda_m^2+\lambda_n^2)-g^2J_0\omega^2(\lambda_m^2+\lambda_n^2)\\ &-J_2g^2\omega^2(\lambda_m^2+\lambda_n^2)^2\}W_{2_{mn}}\\ &=\{C_{12}+C_{12}(\lambda_m^2+\lambda_n^2)\}W_{1_{mn}}\\ &+\{-C_{12}-K_S-K_G(\lambda_m^2+\lambda_n^2)\\ &-g^2K_S(\lambda_m^2+\lambda_n^2)-K_Gg^2(\lambda_m^2+\lambda_n^2)^2\\ &-C_{12}(\lambda_m^2+\lambda_n^2)\}W_{2_{mn}}\end{aligned}$$

(30)

The above two equations can be written in matrix form as:

$$\begin{bmatrix} R_1-R_2\omega^2 & -R_4 \\ -R_4 & R_1-R_2\omega^2 \end{bmatrix}\begin{Bmatrix} W_{1_{mn}} \\ W_{2_{mn}} \end{Bmatrix} = \begin{Bmatrix} 0 \\ 0 \end{Bmatrix} \qquad \textbf{(31)}$$

where

$$\begin{aligned}R_1 = (D+N_{th}g^2)(\lambda_m^2+\lambda_n^2)^2 &+N_{th}(\lambda_m^2+\lambda_n^2)^2+C_{12}+K_S\\ &+K_G(\lambda_m^2+\lambda_n^2)+g^2K_S(\lambda_m^2+\lambda_n^2)\\ &+K_Gg^2(\lambda_m^2+\lambda_n^2)^2+C_{12}(\lambda_m^2+\lambda_n^2)\end{aligned}$$

$$R_2 = J_0+J_2(\lambda_m^2+\lambda_n^2)+g^2J_0(\lambda_m^2+\lambda_n^2)+J_2g^2(\lambda_m^2+\lambda_n^2)^2$$

$$R_4 = C_{12}+C_{12}(\lambda_m^2+\lambda_n^2) \qquad \textbf{(32-a,b,c)}$$

For non-trivial solution of $W_{1_{mn}}$ and $W_{2_{mn}}$, we can get the following determinant as:

$$\begin{vmatrix} R_1-R_2\omega^2 & -R_4 \\ -R_4 & R_1-R_2\omega^2 \end{vmatrix} = 0 \qquad \textbf{(33)}$$

We need to solve this equation for obtaining the natural frequencies. Expanding Eq. (33) we can get the following algebraic equation in natural frequencies of the double layer graphene system:

$$R_2{}^2\omega^4-(R_1R_2+R_2R_3)\omega^2+(R_1R_3-R_4{}^2)=0$$

(34)

The solution of the above equation is obtained as:

$$\omega = \sqrt{\frac{-Z_1 \pm \sqrt{Z_1{}^2-4\,Z_0Z_2}}{2Z_2}} \qquad \textbf{(35)}$$

where

$$Z_2 = R_2{}^2,\quad Z_1 = -(R_1R_2+R_2R_3),\quad Z_0 = R_1R_3-R_4{}^2$$

(36)

The numerical experiments carried out on the SLGS and DLGS are presented and discussed in detail in the next section.

RESULTS AND DISCUSSION

In this paper, the nonlocal plate theory is developed to study the thermal vibration behavior of single and double layer nanoplates. To illustrate the effects of the nonlocal small scale, temperature, mode number and size the non-dimensional natural frequencies are computed and plotted.

A detailed comparison of the present results with the previous results for isotropic case are given in Tables 1, 2 and 3.For comparison of present results with the available literature results (as shown in Table-1), frequency ratio (FR) is defined as

$$\text{FR} = \frac{\omega_{\text{NL}}}{\omega_L} \qquad \textbf{(37)}$$

where ω_{NL} is the natural frequency calculated using nonlocal elasticity theory and ω_{L}

is the frequency calculated using the local elasticity theory.

Properties of the graphene sheet in the validation analysis are considered same as mentioned in the reference [19]. Young's modulus $E = 1.06\,TPa$, Poisson's ratio $\nu = 0.25$, density $\rho = 2250\,kg/m^3$ and thickness, $h = 0.34\,nm$ are calculated. In Table 2, we presented the frequency ratios of the graphene sheet obtained from the present model with the results available in the literature [19]. From Table 2, one could observe that the present results are in good agreement with the results available in the literature [24, 37].

Table 2. Comparison of results for vibration of the graphene sheet for all edges simply supported ($a = 10\,nm$ and $b = 10\,nm$).

$g^2(nm^2)$	FR [18]	FR [19]	FR [*present model*]
0	1	1	1
1	0.9139	0.9139	0.9139
2	0.8467	0.8466	0.8467
3	0.7925	0.7926	0.7925

The free vibration analysis of the single layer graphene sheet performed using present nonlocal plates theory are compared with the molecular dynamics simulation and the generalized differential quadrature results available in ref. [47]. The mechanical properties of graphene sheet considered for this comparisons is Young's modulus E = 1 TPa, Poisson's ratio ν = 0.16, density ρ = 2250 kg/m^3 and thickness h = 0.34 nm. Table 3 show the frequencies obtained using the nonlocalelasticity and the molecular dynamics, while considering the influence of size of the graphene. The dispersive behavior of frequencies in the nonlocal model is clearly observed. However, when larger graphene sheets are considered, the difference between the frequency values diminishes. This is obvious as the size-effects reduce with the increase of size of the single layer graphene. Table 3 give the frequencies of simply-supported zigzag and armchair single layer graphene sheets with different side lengths, respectively. It is evident from the results that armchair sheets generally have relatively higher resonant frequency compared to zigzag sheets of the same dimensions, especially for shorter sheets. It can be observed that the frequencies obtained from the present model are exactly matching with the values presented in ref. [47].

The room or low temperature (i.e., thermal conductivity $\alpha = -1.6 \times 10^{-6}K^{-1}$) and high temperature (i.e., thermal conductivity $\alpha = 1.1 \times 10^{-6}K^{-1}$) used for the nanostructures are considered [48-49]. The temperature change is assumed in the range of $T = 0$ to $90\,K$. The interaction coefficient between two layers C_{12} is given in Table 1, polymer matrix Winkler modulus K_S = 1.13E18 Pa/m and polymer matrix shear modulus K_G = 1.13 Pa/m. Though the value of nonlocal parameter g has not been exactly known for graphene sheet, from literature it is pointed out that value of g should be less than 2 nm.

The fundamental variation of the natural frequency of the single layer graphene sheet obtained from the classical continuum model (g = 0) with the wavenumber n is plotted in Figure 2. It can be observed that the relation between the natural frequency and the mode number is nonlinear. As the wavenumber value increases the value of the fundamental frequency also increases. This is the valid phenomena for all the type of two-dimensional structures [50].

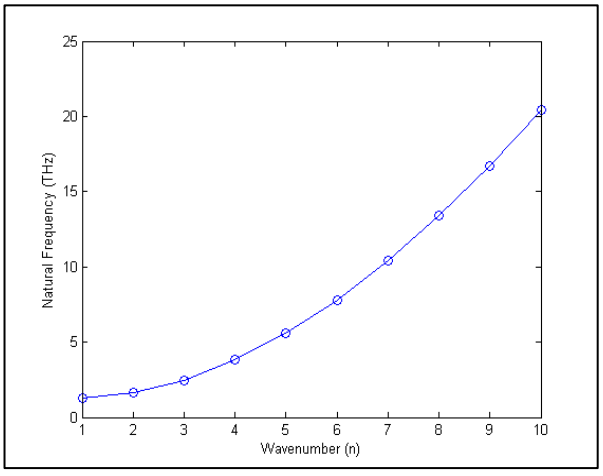

Fig. 2. Variation of the fundamental natural frequency of single layer graphene sheet with the wavenumber obtained from classical plate model.

Table 3. Validation of results for vibration of the armchair and zigzag single-layered graphene sheet for all edges simply supported obtained from molecular dynamics and the nonlocal plate theory (solved via generalized differential quadrature method) available in literature and the present nonlocal plate theory without consideration of thermal and polymer matrix effects.

Size of graphene (*a nm* X *b nm*)	Molecular Dynamics Simulations (THz) [38]		ω for $g^2 = 1.34\ nm^2$ (THz) [38]		ω for $g^2 = 1.34\ nm^2$ (THz) [Present]	
	Armchair	Zigzag	Armchair	Zigzag	Armchair	Zigzag
10 x 10	0.0595014	0.0587725	0.0592309	0.0584221	0.05923	0.05841
15 x 15	0.0277928	0.0273881	0.0284945	0.0202888	0.02845	0.02030
20 x 20	0.0158141	0.0157524	0.0165309	0.0164593	0.01653	0.01646
25 x 25	0.0099975	0.0099840	0.0107393	0.0107085	0.01074	0.01071
30 x 30	0.0070712	0.0070655	0.0075201	0.0075049	0.00752	0.00750
35 x 35	0.0052993	0.0052982	0.0055531	0.0055447	0.00555	0.00555
40 x 40	0.0041017	0.0040985	0.0042657	0.0042608	0.00426	0.00426
45 x 45	0.0032614	0.0032609	0.0033782	0.0033751	0.00338	0.00337
50 x 50	0.0026197	0.0026194	0.0027408	0.0027388	0.00273	0.00274

The effects of the temperature and the mode number (m) on the natural frequency of the single layer graphene sheet are plotted in Figures 3-5 with the mode number (n). The effects of local and nonlocal elasticity are also considered for better comparison. Figures 3-5 are plotted for m = 1 to 3, respectively. It can be observed that all of the natural frequencies become lower with the scale coefficient increasing. Furthermore, for different values of *m*, the natural frequencies at the room or low temperature will be higher than those at the high temperature. As nonlocal scale parameter increases form 0 nm to 1nm, it can be observed that the effect of the temperature is highly dominant and it should be considered for the design of the nanoscale devices that make use of the thermal vibration properties. In these figures it has been observed that the presence of nonlocal scale parameter reduced the natural frequency of the single layer graphene by almost 50% as compared to the classical elasticity. As we further increase the value of the nonlocal scale parameter, say from 0.5 nm to 1.0 nm, is has also been found that the difference is increasing. If we design the nanoscale devices with the results of the classical elasticity, whose results are over estimated (see Figs. 3-5), the design will not lead to satisfy the desirable requirements. It will fail within the half of the frequency band specified. So, it can be concluded that the present nonlocal model is a very efficient and the results are valid, can be used to design and development of the futuristic nanoscale devices. The other important aspect is the influence of the temperature. The classical elasticity, which is a scale free theory, calculations shows that the temperatures effects and are negligible on the natural frequencies of the graphene (Figures 3a, 4a and 5a). The nonlocal elasticity theory shows the temperature effects are predominant as we increase the small scale effects (Figures 3b, 3c, 4b, 4c, 5b and 5c). Such major effects were not captured by the classical theory of elasticity.

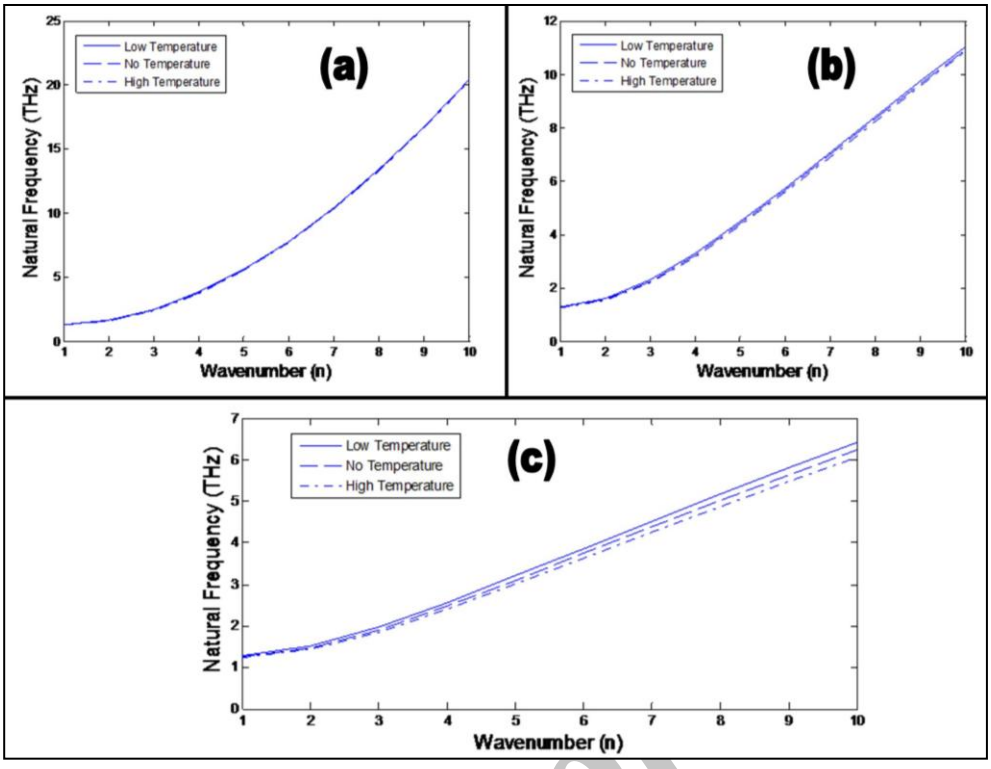

Fig. 3. The variation of natural frequency of single layer graphene with the wavenumber (n) for various temperature effects (low and high) obtained from local and nonlocal elasticity theories and for $m = 1$: (a) $g = 0\ nm$, (b) $g = 0.5\ nm$ and (c) $g = 1.0\ nm$

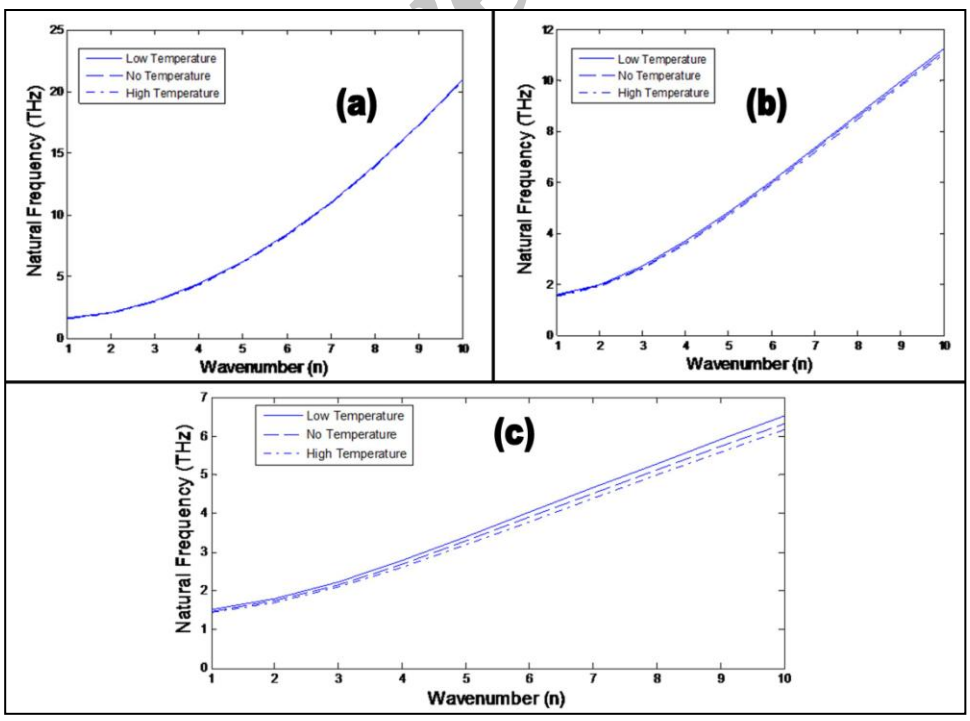

Fig. 4. The variation of natural frequency of single layer graphene with the wavenumber (n) for various temperature effects (low and high) obtained from local and nonlocal elasticity theories and for $m = 2$: (a) $g = 0\ nm$, (b) $g = 0.5\ nm$ and (c) $g = 1.0\ nm$.

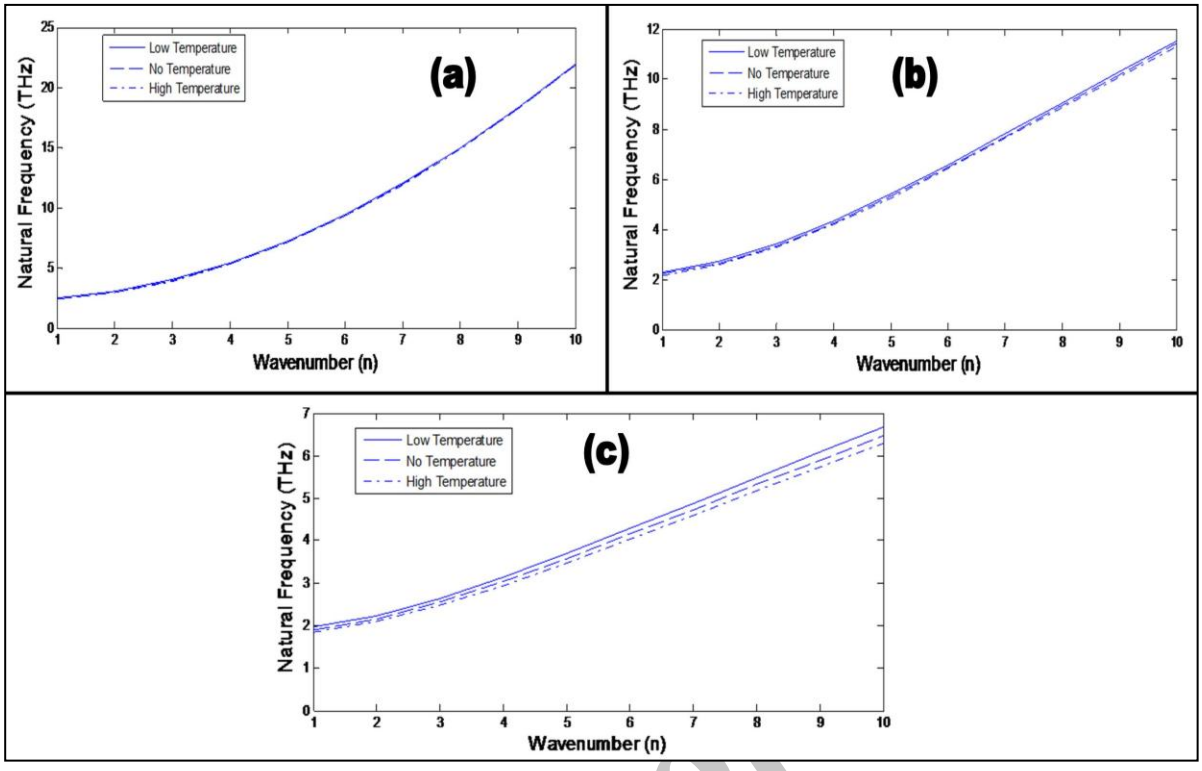

Fig. 5. The variation of natural frequency of single layer graphene with the wavenumber (n) for various temperature effects (low and high) obtained from local and nonlocal elasticity theories and for $m = 3$: (a) $g = 0\ nm$, (b) $g = 0.5\ nm$ and (c) $g = 1.0\ nm$.

The variation of the natural frequency of the single layer graphene sheet with the aspect ratio of ratio of the side lengths of the sheet are plotted in Figure 6. In these figures, the effects of the elastic polymer matrix, temperature, mode number and the nonlocal scale effects are also considered. From Figure 6, it can be observed that the frequency increases with the mode number. As the aspect ratio of the graphene increases the natural frequencies are converging to very small values. Figures 6a and 6b are plotted for the local elasticity calculation without and with matrix effects, respectively. It can be seen that as per the classical elasticity calculation concern, the effect of matrix is not significant on the natural frequencies of the graphene. But from Figures 6c and 6d, it can be observed that the effect of the matrix is significant on the natural frequencies of the graphene because of the cushioning effect onto the graphene. So, it is a serious issue while designing the nanoscale devices. Similar temperature effects are observed as discussed for Figures 3-5.

It is noted when the aspect ratio is less than 1.0, the difference between the vibrational frequencies pertaining to different modes is almost noticeable. But, when the aspect ratio increases, difference between the corresponding values decreases. It implies that the effect of the constraints on the frequencies lowers as if the multi-layered graphene sheet is modeled without any constraints.

Also, the mode shapes illustrated in Figure 7 imply that for the lower fundamental frequency, the adjacent layers move in the same direction, yet for the higher fundamental frequency, the associated mode shapes move in the opposite direction and distort due to the inverse deflections of the adjacent layers. Also, the mode shapes illustrated in Figure 7 corresponding to higher mode numbers render the same results. From Figure 7a to 7d the mode number increases. These mode shape plots are helpful in understanding the deformation behavior of the graphene under dynamic environment. The three-dimensional and the top views of these mode shapes are also given in Figure 7 for clear understanding the phenomena.

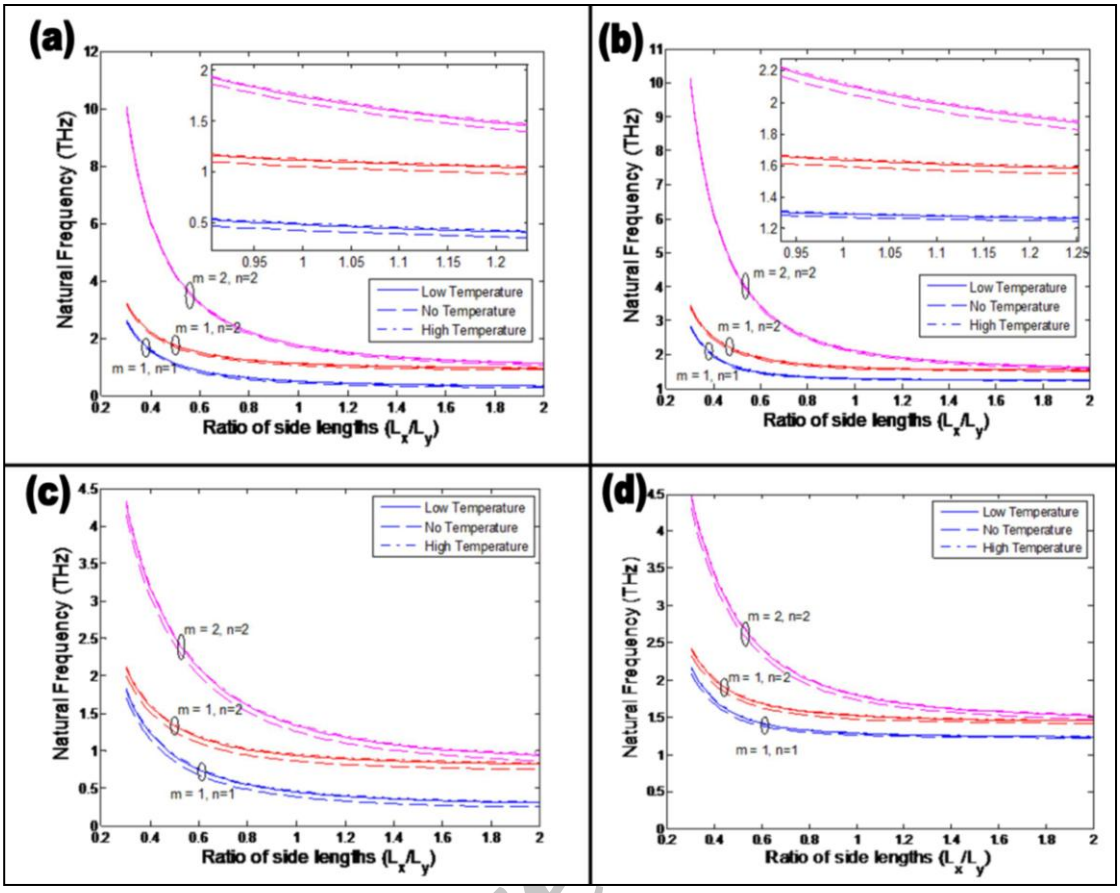

Fig. 6. The variation of natural frequency of single layer graphene with the ratio of the side lengths for various temperature effects (low and high) obtained from local and nonlocal elasticity theories, effect of various mode numbers and the effect of the embedded elastic medium: (a) $g = 0\ nm$ and without matrix, (b) $g = 0\ nm$ and with matrix, (c) $g = 1.0\ nm$ and without matrix and (d) $g = 1.0\ nm$ and with matrix.

The variation of the natural frequencies (ω_1 and ω_2) of the double layer graphene sheet with the aspect ratio of ratio of the side lengths of the sheet are plotted in Figure 8. In these figures, the effects of the mode number and the nonlocal scale effects are also considered. From Figure 8, it can be observed that the frequencies increase with the mode number. As the aspect ratio of the graphene increases the natural frequencies are converging to very small values. Similar matrix effects as obtained for single layer graphene are observed for this case also. So, it is a serious issue while designing the nanoscale devices. It is noted when the aspect ratio is less than 1.2, the difference between the vibrational frequencies pertaining to different modes is almost noticeable. But, when the aspect ratio increases, the difference between the corresponding values are decreases. As the nonlocal scale increases the magnitude of the frequencies decreases as shown in Figure 8a-8c. It also clear from this figure is that the natural frequencies increase as the mode number increases. For higher aspect ratios the difference natural frequencies can be simply neglected.

The effects of the mode numbers (m, n) on the natural frequencies of the double layer graphene are captured in the Figure 9 for local and nonlocal elasticity cases. The classical elasticity calculations show that the frequencies increase with the mode number n, indefinitely as shown in Figure 9a. But the nonlocal elasticity calculations show that the natural frequencies cannot increase indefinitely. Based on the scale parameter the natural frequencies are converging as the mode number n increases as plotted in Figures 9b and 9c. In the same time the magnitude of the frequency is also decreases as the scale parameter become stronger.

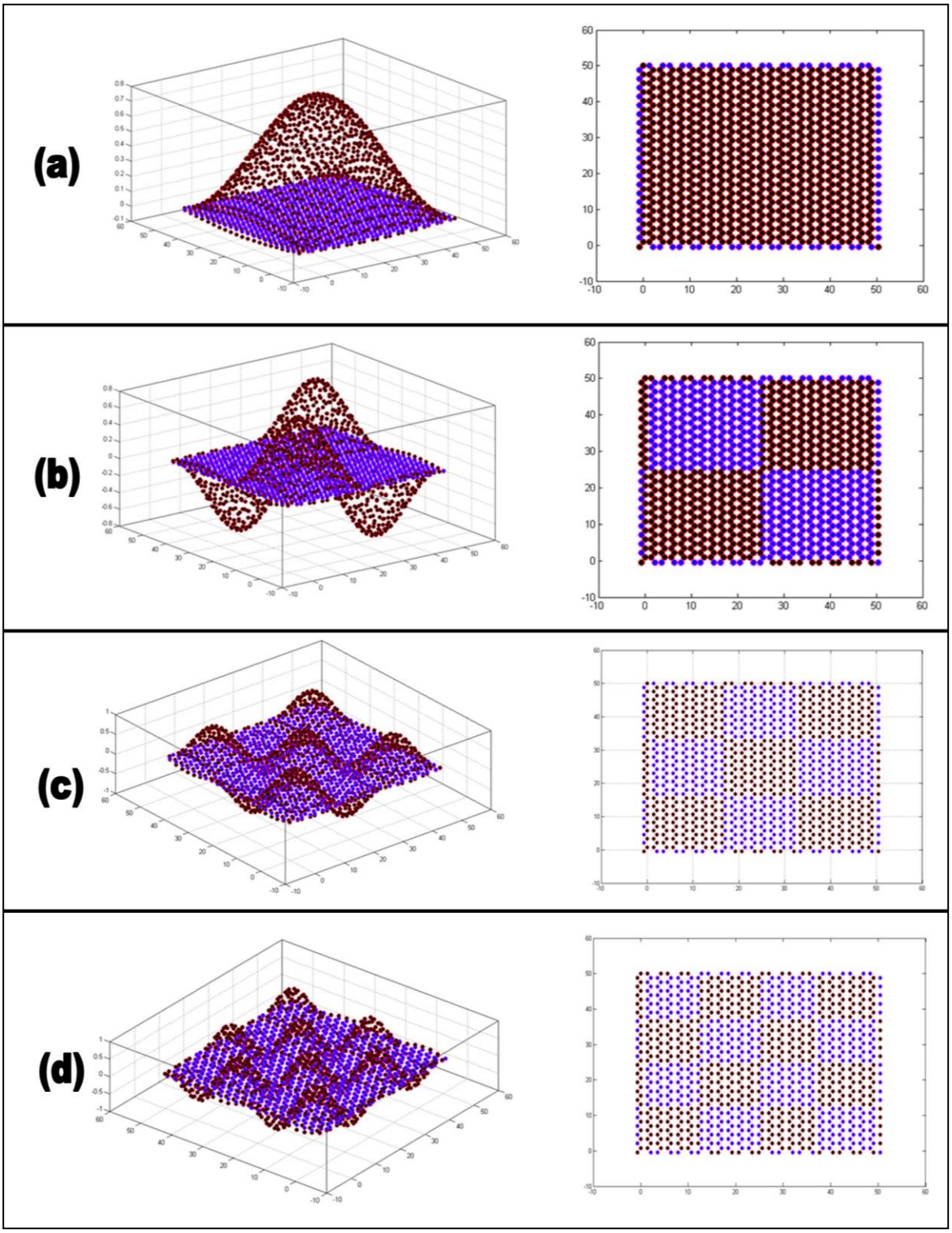

Fig. 7. Mode shapes of the single layer graphene sheet.

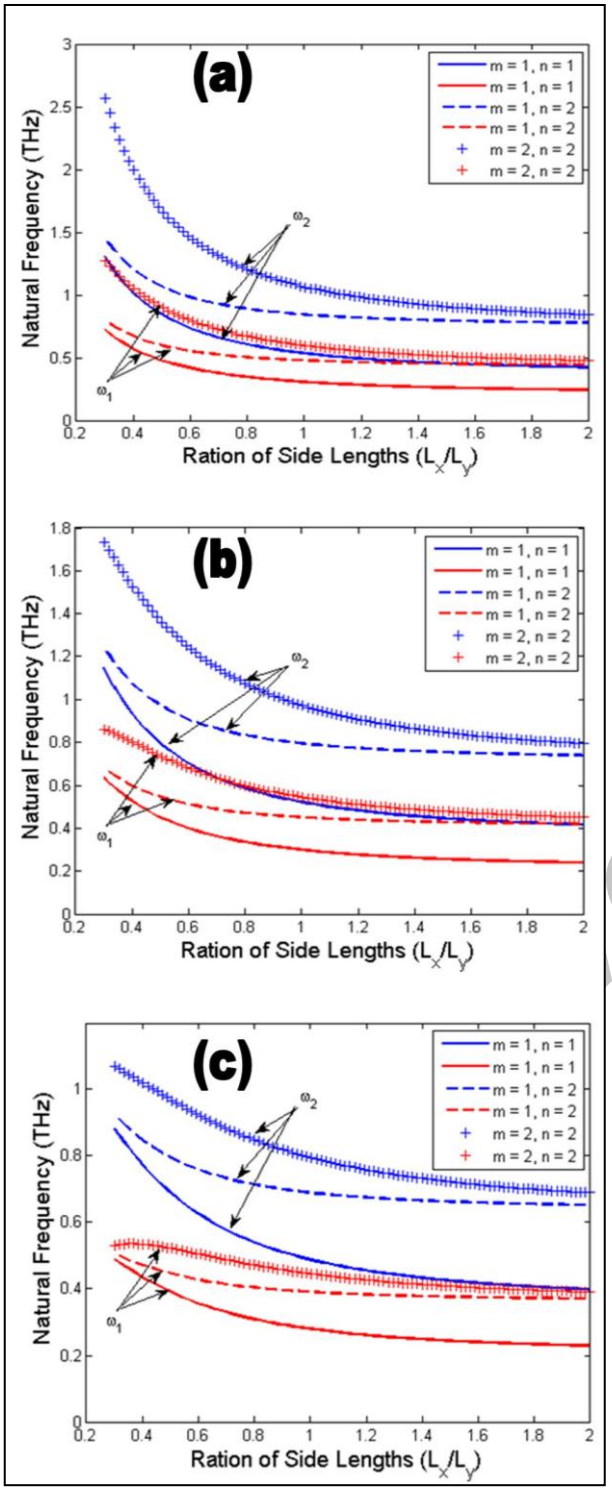

Fig. 8. The variation of natural frequency of double layer graphene with the ratio of the side lengths for various temperature effects (low and high) obtained from local and nonlocal elasticity theories and effect of various mode numbers:
(a) $g = 0\ nm$, (b) $g = 0.5\ nm$ and (c) $g = 1.0\ nm$.

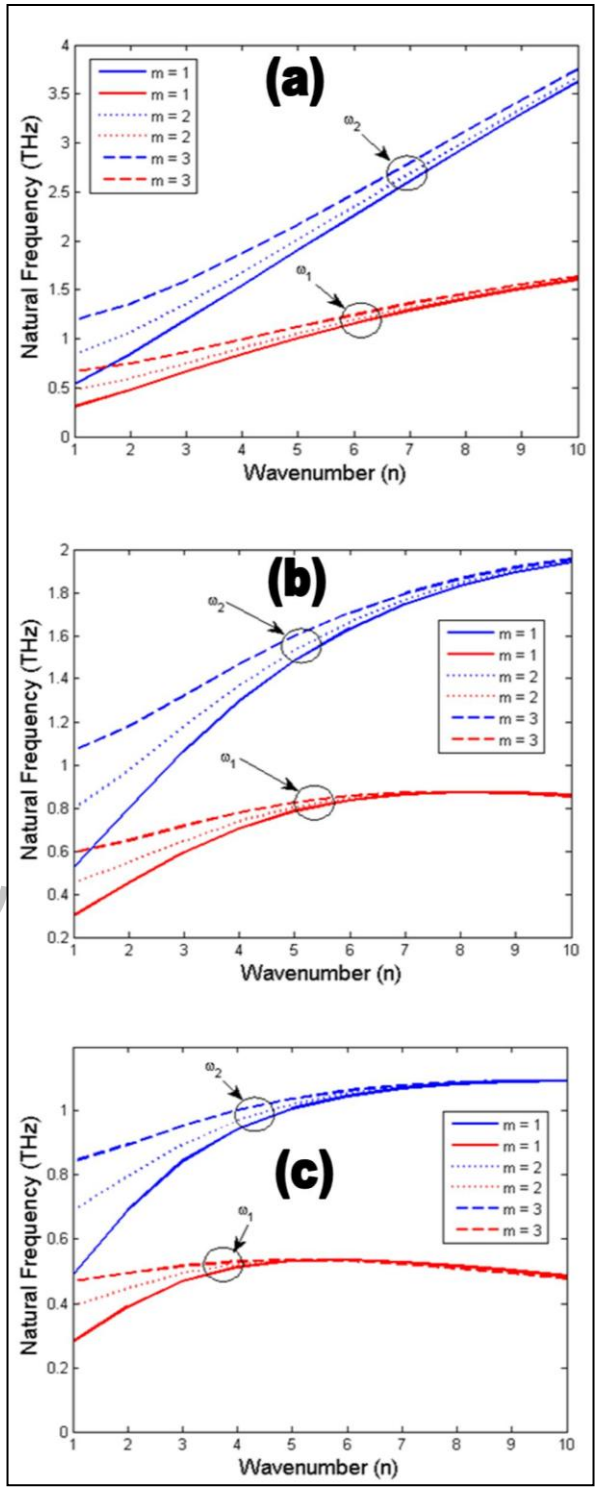

Fig. 9. The variation of natural frequency of double layer graphene with wave number (n) for various mode numbers (m): (a) $g = 0\ nm$, (b) $g = 0.5\ nm$ and (d) $g = 1.0\ nm$.

The temperature effects on the variation of the natural frequencies of the double layer graphene are plotted in Figure 10. It has been found that the temperature effects on the double layer graphene sheet are negligible because of the van der Waals interaction between the layers. The surrounding polymer matrix and the van der Waals interaction made the double layer graphene more stable to external thermal environment. Such results are new and are useful for the design and development of futuristic nano-machines. The nonlocal effects are similar to those discussed in the previous paragraphs.

The first four modes of a double layer graphene are plotted in Figure 11. The undeformed double layer graphene is shown in Figure 11a. Each graphene in double layer graphene system are of 5nm by 5nm is considered for the analysis.

To illustrate the dependence of small scale effect on number of layers, a multilayered graphene sheet with the same properties as described in the previous section has been considered. The sheet is assumed to be free from polymer matrix. It can be clearly observed that nonlocal effect is negligible for 1st mode while it is significant for higher modes. Further nonlocal effect can be seen to be increased with increase in number of layers. This observation can be attributed to the fact that the nonlocal effect for each plate reinforces each other to produce greater nonlocal effect in multilayered graphene sheet.

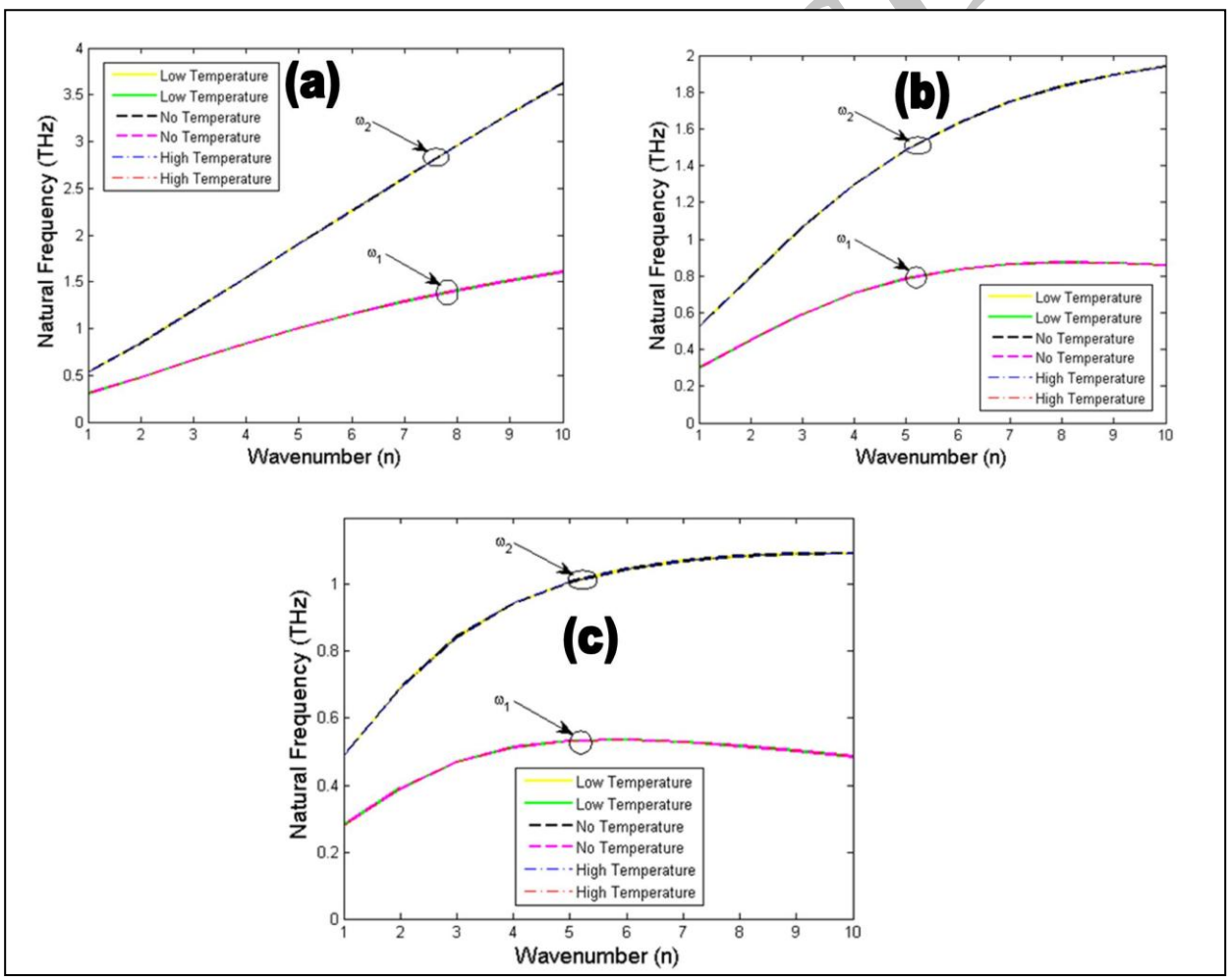

Fig. 10. The variation of natural frequency of double layer graphene with mode number (n) for various temperature effects (low and high) obtained from local and nonlocal elasticity theories (a) $g = 0\ nm$, (b) $g = 0.5\ nm$ and (c) $g = 1.0\ nm$.

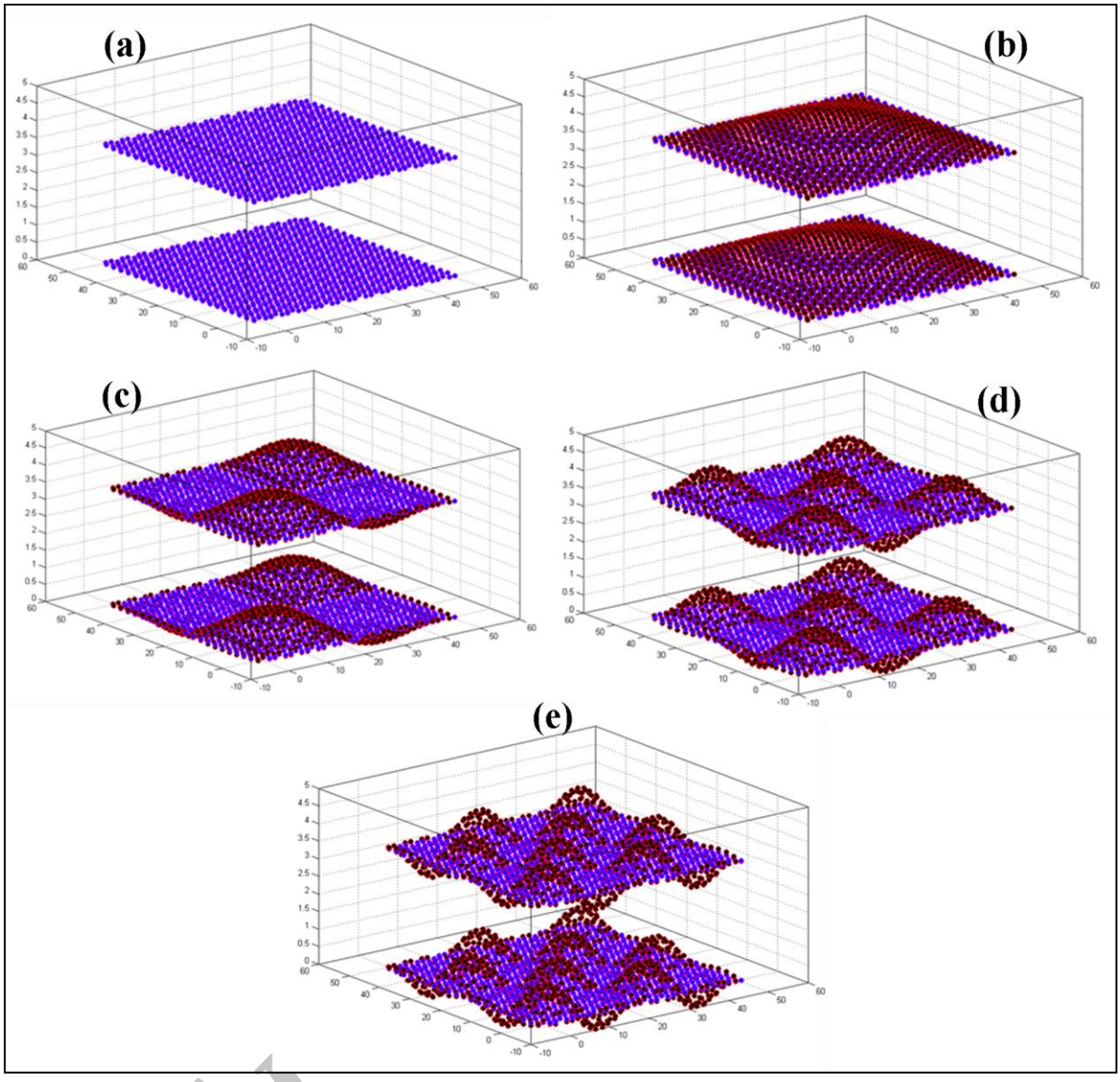

Fig. 11. Mode shapes of double layer graphene sheet

CONCLUSIONS

In this paper, based on the nonlocal continuum model, the thermal effects on the vibration properties of the double-layered nanoplates are studied. The governing equation and the natural frequencies are derived with the axial stress caused by the thermal effects. The influences of the small scales coefficient, the room or low temperature, the high temperature, the half wave number, the temperature change and the width ratio on the vibration behaviors are discussed, respectively. The numerical simulations are performed and it can be concluded that the small scale effects are significant when the wave numbers are larger. Although the temperature change is the same, the natural frequencies are different for the case at the room or low temperature and the high temperature. Furthermore, the behaviors of the frequency ratio are quite different for different modes. This work is expected to be useful to design and analyze the vibration properties of nano scale structures and devices in the nano-electro-mechanical and nano-opto-mechanical systems.

REFERENCES

[1] Thostenson E. T., Ren Z. F., Chou T. W., (2001), Advances in the science and technology of carbon nanotubes and their composites: a review. *Compos Sci Tech*. 61:1899-1912.

[2] Stankovich S., Dikin D. A., Dommett G. H. B., Kohlhaas K. M., Zimney E. J., Stach E. A., Piner R. D., Nguyen S. T., Ruoff R. S., (2006), Graphene-based composite materials. *Nature* 442:282-286.

[3] Ramanathan T., Abdala A. A., Stankovich S., Dikin D. A., Herrera-Alonso M., Piner R. D., Damson D. H., Schniepp H. C., Chen X., Ruoff R. S., Nguyen S. T., Aksay I. A., Rudhomme R. K., Brinson L. C., (2008), Functionalized graphene sheets for polymer nanocomposites. *Nature Nanotech*. 3:327-331.

[4] Han Q., Lu G., (2003), Torsional buckling of a double-walled carbon nanotube embedded in an elastic medium. *Eur J Mech A-Solid*. 22:875–883.

[5] Ru C. Q., (2001), Axially compressed buckling of a double-walled carbon nanotube embedded in an elastic medium. *J Mech Phys Solids*. 49:1265–1279.

[6] Wagner H. D., Lourie O., Feldman Y., Tenne R., (1998), Stress-induced fragmentation of multi-wall carbon nanotubes in a polymer matrix. *Appl Phys Lett*. 72:188–190.

[7] Sakhaee-Pour A., Ahmadian M. T., Vafai A., (2008), Applications of single-layered graphene sheets as mass sensors and atomistic dust detectors. *Solid State Commun*. 4:168–72.

[8] Luo X., Chung D. D. L., (2000), Vibration Damping Using Flexible Graphite. *Carbon*. 38:1499-1515.

[9] Dubay O., Kresse G., (2003), Accurate density functional calculations for the phonon dispersion relations *of* graphite layer and carbon nanotubes. *Phys. Rev. B*. 67:035401.

[10] Xu X., Liao L., (2001), *Mater. Phys. Mech*. 4:148-151.

[11] Horiuchi S., Gotou T., Fujiwara M., Asaka T., Yokosawa T., and Matsui Y., (2004), Single graphene sheet detected in a carbon nanofilm. *Appl. Phys. Lett*. 84:2403-2413.

[12] Behfar K., Naghdabadi R., (2005), Nanoscale vibrational analysis of a multi-layered graphene sheet embedded in an elastic medium. *Compos Sci Technol*. 65:1159–1164.

[13] Behfar K., Seifi P., Naghdabadi R., Ghanbari J., (2006), An Analytical Approach to Determination of Bending modulus of a Multi-Layered Graphene Sheet. *Thin Solid Films*. 496(2):475–480.

[14] Kitipornchai S., He X. Q., Liew K. M., (2005), Continuum model for the vibration of multilayered graphene sheets. *Phys. Rev. B*. 72:075443.

[15] Qian D., Wagner G. J., Liu W. K., Yu M. F., Ruoff R. S., (2002), Mechanics of carbon nanotubes. *Appl Mech Rev*. 55:495–533.

[16] Ru C. Q., (2004), Elastic models for carbon nanotubes. In: Nalwa HS (Ed.), Encyclopedia of Nanoscience and Nanotechnology. *American Scientific Publishers*. 2:731–744.

[17] Peddieson J., Buchanan G. R., McNitt R. P., (2003), Application of nonlocal continuum models to nanotechnology. *Int J Eng Sci*. 41:305–312.

[18] Pradhan S. C., Phadikar J. K., (2009), Small scale effect on vibration of embedded multilayered graphene sheets based on nonlocal continuum models. *Phys Lett A*. 373:1062-1069.

[19] Pradhan S. C., Phadikar J. K., (2009), Nonlocal elasticity theory for vibration of nanopaltes. *J Sound Vib*. 325:206-223.

[20] Ansari R., Sahmani S., Arash B., (2010), Nonlocal plate model for free vibrations of single-layered graphene sheets. *Phys Lett A*. 375:53-62.

[21] Pradhan S. C., Kumar A., (2011), Vibration analysis of orthotropic graphene sheets using nonlocal elasticity theory and differential quadrature method. *Compos Struct*. 93:774-779.

[22] Narendar S., Gopalakrishnan S., (2012), Scale effects on buckling analysis of orthotropic nanoplates based on nonlocal two-variable refined plate theory. *Acta Mech*. 223(2):395-413.

[23] Narendar S., Gopalakrishnan S., (2012), Nonlocal flexural wave propagation in an embedded graphene. *Int. J Comp*. 6(1):29-36.

[24] Narendar S., Gopalakrishnan S., (2012), Temperature effects on wave propagation in nanoplates. *Comp. Part B: Engg*. 43:1275–1281.

[25] Narendar S., (2011), Buckling of micro/nanoscale plates using the two variable refined plate theory incorporating nonlocal small scale effects. *Comp. Struct*. 93:3093–3103.

[26] Narendar S., Roy Mahapatra D., Gopalakrishnan S., (2011), Ultrasonic wave characteristics of a monolayer graphene on silicon substrate. *Comp. Struct*. 93:1997-2009.

[27] Narendar S., Roy Mahapatra D., Gopalakrishnan S., (2010), Investigation of the

effect of nonlocal scale on ultrasonic wave dispersion characteristics of a monolayer graphene. *Comp. Mate. Scie*. 49:734-742.
[28] Narendar S., Gopalakrishnan S., (2010), Strong nonlocalization induced by small scale parameter on terahertz flexural wave dispersion characteristics of a monolayer graphene. Physica E: Low-dimen. Sys. *Nanostruct*. 43:423-430.
[29] Narendar S., Gopalakrishnan S., (2012), Scale effects on ultrasonic wave dispersion characteristics of a monolayer graphene embedded in elastic medium. *J. Mech. of Mat. and Struct*. in production.
[30] Narendar S., Gopalakrishnan S., (2012), Ultrasonic flexural wave dispersion characteristics of a monolayer graphene embedded in polymer matrix based on nonlocal continuum mechanics. *Comp. Part B*: Engg. http://dx.doi.org/10.1016/j.compositesb.2012.04.058 *in press*.
[31] N. Satish, Narendar S., Gopalakrishnan S., (2012), Thermal vibration analysis of orthotropic nanoplates based on nonlocal continuum mechanics. *Physica E: Low-dimen. Sys. Nanostruct*. 44:1950–1962.
[32] Sharma P., Ganti S., Bhate N., (2003), Effect of surfaces on the size-dependent elastic state of nano-in-homogeneities. *Appl Phys Lett*. 82:535–537.
[33] Sun C. T., Zhang H., (2003), Size-dependent elastic moduli of plate like nanomaterials. *J Appl Phys*. 93:1212.
[34] Eringen A. C., (2002), Nonlocal continuum field theories. New York (NY): *Springer*.
[35] Eringen A. C., Edelen D. G.B., (1972), On non-local elasticity. *Int J Eng Sci*. 10:233-240.
[36] [36] Eringen A. C., (1972), Linear theory of non-local elasticity and dispersion of plane waves. *Int J Eng Sci*. 10:425-435.
[37] Chen Y., Lee J. D., Eskandarian A., (2004), Atomistic viewpoint of the applicability of micro-continuum theories. *Int J Solids Struct*. 41:2085–2097.
[38] Sudak L. J., (2003), Column buckling of multi-walled carbon nanotubes using nonlocal continuum mechanics. *J. Appl. Phys*. 94:7281–7287.
[39] Zhang Y. Q., Liu G. R., Xie X. Y., (2005), Free transverse vibration of double-walled carbon nanotubes using a theory of nonlocal elasticity. Phy. *Review B*. 71:195404.
[40] Sears A., Batra R. C., (2004), Macroscopic properties of carbon nanotubes from molecular mechanics simulations. *Phys. Review* B. 69:235406.
[41] Wang L. F., Hu H. Y., Guo W. L., (2006), Validation of the non-local elastic shell model for studying longitudinal waves in single-walled carbon nanotubes. *Nanotech*. 17:1408–1415.
[42] Wang Q., (2005), Wave propagation in carbon nanotubes via nonlocal continuum mechanics, *J. Appl. Phys*. 98:124301.
[43] Narendar S., Roy Mahapatra D., Gopalakrishnan S., (2011), Prediction of nonlocal scaling parameter for armchair and zigzag single-walled carbon nanotubes based on molecular structural mechanics, nonlocal elasticity and wave propagation. *Int. J. Eng*. Scie. 49:509–522.
[44] Narendar S., Gopalakrishnan S., (2012), A nonlocal continuum mechanics model to estimate the material property of single-walled carbon nanotubes. *Int. J. Nanosci*. 11(1):1250007.
[45] Liew K. M., He X. Q., Kitipornchai S., (2006), The effect of Van der Waals interaction modeling on the embedded in an elastic matrix. *Acta Mater*. 54:4229-4237.
[46] Reddy J. N., (1997), Mechanics of Laminated Composite Plates, Theory and Analysis. Chemical Rubber Company, *Boca Raton, FL*.
[47] Ansari R., Sahmani S., Arash B., (2010), Nonlocal plate model for free vibrations of single-layered graphene sheets. *Physics Lett. A*. doi:10.1016/j.physleta.2010.10.028.
[48] Zhang Y. Q., Liu X., Liu G. R., (2007), Thermal effect on transverse vibrations of double- walled carbon nanotubes. *Nanotech*. 18:445701.
[49] Lee H. L., Chang W. J., (2009), A closed-form solution for critical buckling temperature of a single-walled carbon nanotube. *Physica E*. 41:149-154.
[50] Rao S. S., (2011), Mechanical Vibrations. Prentice-Hall, *Upper Saddle River, NJ*.

Cite this article as: T. J. Prasanna Kumar *et al.*: Thermal vibration analysis of double-layer graphene embedded in elastic medium based on nonlocal continuum mechanics.
Int. J.Nano Dimens. 4(1): 29-49, Summer 2013